Remnant Fermi Surface in the Presence of an Underlying Instability in Layered 1T-TaS$_2$

Th. Pillo,[1] J. Hayoz,[1] H. Berger,[2] M. Grioni,[2] L. Schlapbach,[1] and P. Aebi[1]

[1]*Institut de Physique, Université de Fribourg, CH-1700 Fribourg, Switzerland*
[2]*Institut de Physique Appliquée, EPF, CH-1015 Lausanne, Switzerland*

We report high resolution angle-scanned photoemission and Fermi surface (FS) mapping experiments on the layered transition-metal dichalcogenide 1T-TaS$_2$ in the quasicommensurate (metallic) and the commensurate (insulating) charge-density-wave (CDW) phase. Instead of a nesting induced partially removed FS in the CDW phase we find a pseudogap over large portions of the FS. This remnant FS exhibits the symmetry of the one-particle normal state FS. Possibly, this Mott localization induced transition represents the underlying instability responsible for the pseudogapped FS.

Very recently Fermi surface (FS) measurements using angle-resolved photoemission (ARPES) have gained particular interest with respect to the mechanism behind high-temperature superconductivity [1,2]. In underdoped cuprates a remnant FS [3] has been detected at temperatures around the transition temperature T_c [2]. The important point seems to be that there is an underlying electronic instability which drives the pseudogap [4] and the remnant FS behavior [5,6]. One might ask whether to expect a comparable behavior of the FS for other materials with underlying electronic phase transitions. As a possible candidate appears 1T-TaS$_2$, which has as an underlying instability the Mott localization derived transition at 180 K, where the symmetry does not change [7].

The layered transition metal dichalcogenide 1T-TaS$_2$ is a model system being the first material where charge density waves (CDW) have been experimentally discovered by means of superlattice spots in x-ray diffraction (XRD) experiments [8]. It provides, however, one crucial difference to other isostructural 1T-type materials, because it shows a Mott localization induced transition at 180 K, where electrons stemming from the Ta 5d-band manifold become more and more localized with decreasing temperature and, suddenly, yield a commensurate locked-in CDW and an insulating state [7]. The relevant phases here are, first, the quasicommensurate (QC) CDW phase, stable at room temperature (RT) and known to exhibit hexagonal arrays of commensurate domains with ($\sqrt{13} \times \sqrt{13}$) symmetry [9]. Second, the commensurate (C) CDW phase below 180 K where the CDW is locked in.

In the present Letter we show, using temperature dependent *scanned* ARPES and FS mapping (FSM) measurements on 1T-TaS$_2$ that the FS at room temperature is pseudogapped, although at most a partial removal of the FS due to nesting is expected. It remains a *remnant* FS yielding the symmetry of the normal (metallic) state (NS) even below 180 K with residual spectral weight at the Fermi level E_F.

Experiments have been performed in a modified VG ESCALAB Mk II spectrometer using monochromatized

He-Iα (21.2 eV) photons [10]. The FSM measuring mode including sequential motorized sample rotation has been outlined previously [11]; i.e., spectral weight at E_F is mapped as a function of $\mathbf{k}_\parallel$, the parallel component of the electron wave vector, throughout the BZ. Note that this type of *scanned* ARPES measurement yields *direct* information about relevant points in $\mathbf{k}$ space, in contrast to traditional ARPES work, where the data sets are intrinsically smaller and possibly omit information. ARPES and FSM experiments were performed with energy and angular resolution of 30 meV and $\pm 0.5°$, respectively [12].

Pure 1T-TaS$_2$ samples were prepared by vapor transport [13,14] and cleaved *in situ* at pressures in the upper 10^{-11} mbar region. Surface quality and cleanness were checked by low energy electron diffraction (LEED) and x-ray photoelectron spectroscopy, respectively. Before and after each experiment the valence band spectrum was checked to ensure sample quality. Measurements were done on different samples and cleavages assuring perfect reproducibility. In both, the QC- and the C-phase, LEED shows the well-defined superspots characteristic for the $\sqrt{13} \times \sqrt{13}$ symmetry. X-ray photoelectron diffraction [15] allowed us to determine the sample orientation *in situ* with an accuracy of better than 0.5°.

Figure 1 shows FSM data of 1T-TaS$_2$ taken with $h\nu = 21.2$ eV in the QC-phase (a) and in the C-phase (b). The (1×1), i.e., NS-surface Brillouin zones (SBZ) are given by the hexagons with the corresponding high symmetry points indicated. Additionally, in panel (b) the (expected) new SBZ due to the commensurate CDW is illustrated by the small hexagons. The raw data have been normalized [16] such that the overall polar intensity variation has been removed and symmetrized according to the space group D_{3d}^3 [17] of the CdI$_2$-type materials. In all panels the measurements are given in a parallel-projected (linear in $\mathbf{k}_\parallel$) linear gray scale representation with maximum intensity corresponding to white. The center of the plots denotes normal emission (Γ, polar emission angle $\theta = 0°$) and the outer circle represents grazing emission ($\theta = 90°$). Elliptic branches, centered around M, as expected from
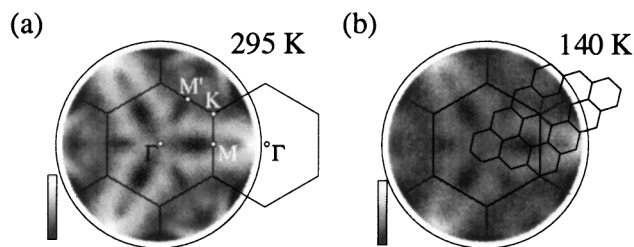
FIG. 1. Fermi surface mapping results of 1T-TaS$_2$, taken with monochromatized He-Iα radiation (21.2 eV). Map (a) has been obtained at room temperature, i.e., in the quasicommensurate CDW phase. Map (b) was measured at 140 K, in the commensurate CDW phase. The raw data have been normalized according to the space group symmetry [13] in order to enhance contrast (see text).

band-structure calculations [18] are seen. A comparable shape has been found in a dichroism study of the valence band of 1T-TaS$_2$ [19].

When comparing the data at 295 and 140 K, two features are surprising. First, at 295 K as well as at 140 K, the symmetry is threefold and not broken according to the ($\sqrt{13} \times \sqrt{13}$) reconstruction as indicated by the small hexagons in panel (b) and as seen from LEED. This might be explained by a small Fourier component of the CDW potential [20], at least for 295 K. Nevertheless, this is surprising since 1T-TaS$_2$ is reported to have a very strong CDW amplitude [9,17]. Another explanation may be that self-energy effects broaden the spectral function such that the $\sqrt{13}$ features are obscured. Furthermore, LEED essentially probes the ion core potential, whereas ARPES senses the wave functions. Second, for 140 K, one would not expect to see any FS at all due to the reported rigid quasiparticle (QP) band shift of 180 meV in the C-phase [21]. Instead we observe small but finite spectral weight at E_F all over the "FS."

In order to get more detailed information about the actual behavior of the FS, ARPES spectra were measured along the FS contour. Spectra are given in Fig. 2 for 295 and 140 K, respectively. The arrow on the right side indicates the **k**-space locations of the spectra 1–41 as displayed in Fig. 3 (bottom) where the NS-FS is mimicked by ellipses. For 295 K one observes two broad QP peaks (Fig. 2), denoted A and B in the spectra at energy positions of about 220 and 700 meV, respectively. Both peaks show significant modulation along the FS contour but practically no dispersion. Most importantly, there is no clear Fermi edge visible. Instead, we observe a leading edge shifted of at least 30 meV as compared to the Fermi edge of the polycrystalline Cu sample holder. We interpret this in terms of a pseudogap. The pseudogap remains open all over the FS, indicating that there is no clear E_F crossing of a QP. Instead one has a *remnant* Fermi surface (RFS) already at room temperature [22].

In the low temperature C-phase spectra (right panel) along the FS contour the situation is very similar except
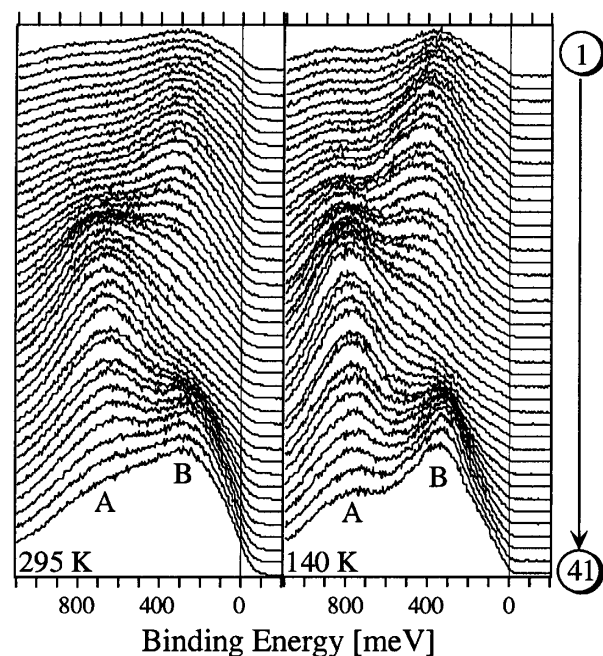

FIG. 2. ARPES spectra (raw data) along the Fermi surface contour, performed at room temperature (left side) and at 140 K (right side). Enumeration of spectra is shown at the right by the arrow, corresponding to the drawing in Fig. 3. The two quasiparticle peaks A and B are explained in the text.

that both peaks yield a rigid shift of about 120 meV and become narrower. Despite the energy shift the gap does not open completely and the ARPES spectra retain small but finite spectral weight at E_F. Note that in Fig. 1(b) the same **k**-space distribution is observed as in Fig. 1(a), however, with the maximal intensity reduced by approximately an order of magnitude. This means that the QC-C transition does not change the symmetry of the FS.

For convenience, Fig. 3 shows a sketch of the one-particle NS Ta $5d$ band with the Fermi level crossing as expected from a one-particle calculation of the CDW-free phase at about $1/3$ of the ΓM distance [18,23–26]. The "shady" areas indicate the practically dispersionless subbands arising from the CDW potential splitting the Ta $5d$ band [7,23]. ARPES investigations have given experimental evidence [13,14,21] for a so-called "star-of-David" model of Fazekas and Tosatti [7]. Thirteen Ta atoms form two outerlying bonding shells with six Ta atoms each, displayed in ARPES spectra as the two low energetic manifolds. The shallow band containing the remaining thirteenth electron is susceptible to a Mott localization and splits into a lower occupied (LHB) and upper unoccupied Hubbard subband. The LHB is manifest as a sharp, dispersionless peak near E_F in near-normal emission ARPES spectra of the C-phase [13,14,21].

Figure 3 also displays the $k_\parallel(E_F)$ of the NS-FS and, by interrupting the solid lines, highlights the region around the small half-axis of the ellipse where it is susceptible for nesting. Since the loss of intensity of peak B appears
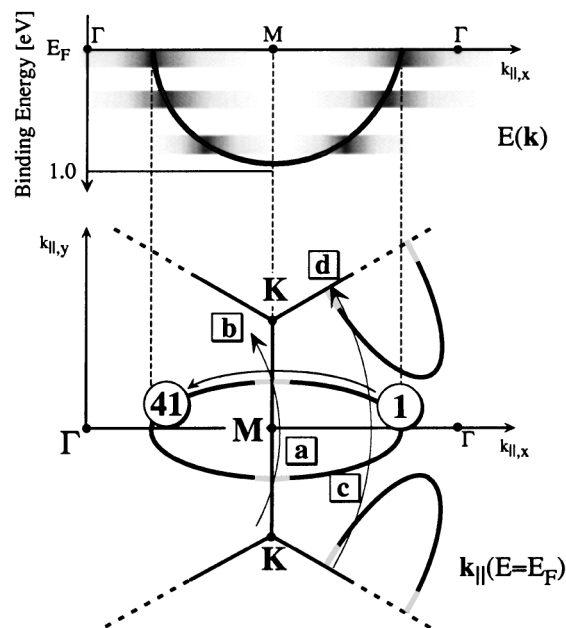
FIG. 3. Simplifying sketch of the band dispersion and the Fermi surface in $1T$-TaS_2 as expected from a one-particle calculation. The upper panel mimics the $E(\mathbf{k})$ dispersion of the unperturbed Ta $5d$ band in the ΓM azimuthal direction. The CDW induced subbands are indicated by the shady areas. The lower panel sketches the inverse situation, the $\mathbf{k}_\parallel(E = E_F)$ dispersion, i.e., the Fermi surface, built up by the elliptic shape of the Ta $5d$ band. The arc along the FS ellipse denotes the location in $\mathbf{k}$ space where the ARPES spectra of Fig. 2 have been measured. The two circular arcs show where the ARPES spectra of Fig. 4 have been measured.

exactly in this region (Fig. 2), it may be attributed to removal of spectral weight due to the Peierls gap [26]. From Fig. 2 it is now clear that the FS is disrupted to a RFS yet retains the overall NS symmetry even below 180 K.

In order to corroborate the observation of a pseudogap along the RFS contour probed in Fig. 2, we measured azimuthal ARPES spectra along the two circular arcs shown in Fig. 3, i.e., along $a \rightarrow b$ and $c \rightarrow d$. Results for RT are shown in Figs. 4(a) and 4(b), respectively. Figure 4(a) shows the spectra for a polar angle of 32° ($a \rightarrow b$), thus crossing the Peierls gap region as indicated in Fig. 3. Figure 4(b) shows the spectra for a polar angle of 50° ($c \rightarrow d$), being outside the region influenced by the CDW. In both panels we display a gray scale representation and the spectra. The arrows indicate the Fermi level crossing of the NS band as obtained from plots of the occupation number $n(\mathbf{k})$. In both panels a single dispersing band can be seen sitting on an incoherent background which is built from nondispersing QP peaks, corresponding to the decay of the NS band into three submanifolds [7]. At $\theta = 32°$ polar angle, the dispersing band reaches down to 0.95 eV binding energy in the $[\Gamma M]$ azimuth, and for $\theta = 50°$ we have 0.5 eV as the maximum binding energy. The maximum binding energies fit well with the fact that the $a \rightarrow b$ scan crosses at the full
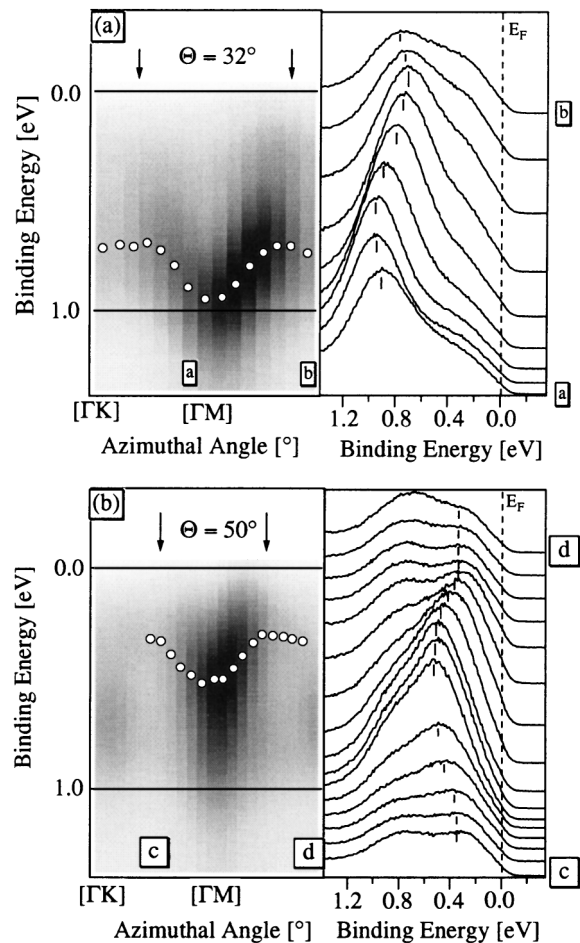

FIG. 4. (a) Room temperature ARPES spectra measured along the circular arcs sketched in Fig. 3, i.e., with two "FS" crossings, for a polar angle of $\theta = 32°$. $\mathbf{K}$-space azimuths are indicated at the bottom. The arrows indicate the Fermi surface crossings from the $n(\mathbf{k})$ analysis (see text). In the spectra $a \rightarrow b$ on the right the dispersing quasiparticle peak is indicated by small ticks. (b) ARPES spectra as in (a), but at $\theta = 50°$ polar angle, i.e., outside the Peierls gap region (disrupted region on the ellipse). As in (a), spectra are shown in the right panel from c to d, as indicated in the gray-scale plot and in Fig. 3.

depth of the band near M (see Fig. 3), whereas the $c \rightarrow d$ scan probes a shallower part near the end of the ellipse. As a guide to the eye, the peak positions are shown, respectively, as white circles overplotted on the gray scale map and as small ticks in the spectra. Strikingly, one can see the backdispersing of the band when it reaches the region indicated by the arrows. However, there is *no* QP band crossing the Fermi level anywhere in the irreducible BZ wedge confirming that the original FS is completely pseudogapped and remains a RFS.

These findings are remarkable because in the CDW phase above the localization induced Mott transition one would expect an intact FS with partially removed portions due to nesting, either via large parallel areas (i.e., the interrupted portion of the ellipse; bottom of Fig. 3) of the

NS-FS or via a strong electron-phonon coupling constant. And yet we are left with a remnant FS. From XRD [8] and LEED [27] we do not expect other nested FS regions than those indicated by the missing parts of the ellipse in Fig. 3.

Originally the lattice distortion may be driven by nesting, but the electronic structure is more and more influenced as the localization of star-centered Ta electrons sets in. The QC-phase exhibits commensurate domains with an incoherent superposition of domains. Hence, the overlap of the QP peaks is considerable but decreases with temperature [20]. At the QC-C transition there is probably a sudden increase of U_{dd} (the Coulomb repulsion between d electrons on neighboring "star" centers) which pops the two Hubbard subbands apart. The pseudogap may therefore be interpreted as due to finite, temperature dependent hybridization of the overlapping tails of the two Hubbard subbands. Interestingly, the remaining spectral weight distribution keeps the same symmetry.

From Fig. 4 we note that at RT we are left with *one* dispersing QP band, whereas the other two bands are visible as shoulders in the QP peak, and already exhibit a dispersionless behavior and therefore localized character. This clearly indicates the presence of a type of precursor at RT of the underlying Mott transition at 180 K and may be the origin of the absence of a "real" FS.

There is similarity with underdoped cuprates [2,5,6] where a crossover temperature scale $T^* > T_c$ has been introduced [5]. Between T^* and T_c a pseudogap opens gradually [at least away from $(\pi, 0)$] with decreasing temperature. At T_c then, the leading edge of the spectral function is fully retracted and a coherent QP peak appears. This is quite similar to what happens here. One is, therefore, tempted to introduce such a T^* as well for $1T$-TaS$_2$, i.e., at the onset of the localization where the CDW becomes quasicommensurate. At RT we are between T^* and T_c and have a pseudogap, i.e., spectral weight at E_F but no transition through E_F. Below 180 K, i.e., T_c, the leading edge is fully retracted and a QP peak appears.

In summary, we have shown by means of temperature dependent scanned ARPES and FSM measurements that at room temperature $1T$-TaS$_2$ exhibits a remnant FS. This FS is not only affected by a comparingly small influence of the CDW formation, i.e., nesting. Rather, it is the underlying Mott localization induced transition which seems to tune the FS properties. This remnant FS is retained (with reduced spectral weight) even below the QC-C transition with the same symmetry as in the metallic normal state phase. As in the underdoped cuprates, the underlying transition influences the electronic structure well above the temperature where coherence sets in.

[1] F. Ronning *et al.,* Science **282**, 2067 (1998).
[2] M. R. Norman *et al.,* Nature (London) **392**, 158 (1998).
[3] A remnant Fermi surface in ARPES may be understood as the momentum distribution of spectral weight following that of the normal "metallic" state, despite the fact that there is no quasiparticle crossing the Fermi energy E_F.
[4] A pseudogap is inferred from ARPES if a quasiparticle peak is approaching E_F without the midpoint of its leading edge ever reaching E_F.
[5] H. Ding *et al.,* Phys. Rev. Lett. **78**, 2628 (1997).
[6] H. Ding *et al.,* Nature (London) **382**, 51 (1996).
[7] P. Fazekas and E. Tosatti, Philos. Mag. B **39**, 229 (1979); Physica (Amsterdam) **99B**, 183 (1980).
[8] J. A. Wilson *et al.,* Phys. Rev. Lett. **32**, 882 (1974).
[9] X. Wu *et al.,* Science **243**, 1703 (1989); B. Giambattista *et al.,* Phys. Rev. B **41**, 10 082 (1990); W. Han *et al., ibid.* **48**, 8466 (1993); B. Burk *et al.,* Phys. Rev. Lett. **66**, 3040 (1991); X. Wu *et al., ibid.* **64**, 1150 (1990).
[10] Th. Pillo *et al.,* J. Electron Spectrosc. Relat. Phenom. **57**, 243 (1998).
[11] P. Aebi *et al.,* Phys. Rev. Lett. **72**, 2757 (1994); T. J. Kreutz *et al.,* Phys. Rev. B **58**, 1300 (1998); Th. Straub *et al.,* Phys. Rev. B **55**, 13 473 (1997).
[12] Analogous experiments were also done with He-IIα (40.8 eV) and H Lyα (10.2 eV) radiation, implying different matrix elements and $\mathbf{k}_\perp$ locations, confirming the results shown below for He-Iα.
[13] B. Dardel *et al.,* Phys. Rev. B **45**, 1462 (1992).
[14] B. Dardel *et al.,* Phys. Rev. B **46**, 7407 (1992).
[15] J. Osterwalder *et al.,* Phys. Rev. B **44**, 13 764 (1991).
[16] Normalization is achieved by dividing intensities on each azimuthal scan, i.e., concentric circle around Γ, by its mean intensity.
[17] J. A. Wilson *et al.,* Adv. Phys. **24**, 117 (1975).
[18] A. M. Woolley and G. Wexler, J. Phys. C **10**, 2601 (1977); H. W. Myron and A. J. Freeman, Phys. Rev. B **11**, 2735 (1975).
[19] T. Matsushita *et al.,* Phys. Rev. B **56**, 7687 (1997).
[20] R. Claessen *et al.,* Phys. Rev. B **41**, 8270 (1990).
[21] R. Manzke *et al.,* Europhys. Lett. **8**, 195 (1989).
[22] It is unlikely that matrix elements are responsible for the small spectral weight at E_F since a few hundred meV away the spectral weight is strong again and matrix elements in this kinetic energy range are not expected to exhibit such a strong energy dependence. Likewise, we do not expect a rapid variation as a function of $\mathbf{k}_\parallel$ such as to show up as pronounced lines. Furthermore, the use of other photon energies (He-IIα, H Lyα) confirms that matrix element or $\mathbf{k}_\perp$ effects do not affect our results.
[23] N. V. Smith *et al.,* J. Phys. C **18**, 3175 (1985).
[24] R. Manzke *et al.,* J. Phys. C **21**, 2399 (1988).
[25] F. Zwick *et al.,* Phys. Rev. Lett. **81**, 1058 (1998).
[26] Th. Pillo *et al.* (to be published).
[27] Th. Pillo *et al.,* J. Electron Spectrosc. Relat. Phenom. **101–103**, 811 (1999).